JOURNAL OF SOLID STATE CHEMISTRY 96, 169–180 (1992)

Anionic Polymeric Bonds in Transition Metal Ditellurides

S. JOBIC, R. BREC, AND J. ROUXEL

Laboratoire de Chimie des Solides, Institut des Matériaux de Nantes,
44072, Nantes Cédex 03, France

Received July 12, 1991

Whereas sulfur and selenium tend, in some dichalcogenides, to bond to give $(X_2)^{2-}$ or $(X_2)^{-}$ pairs, tellurium is more prone to setting multiple bonds. Reported CdI_2-like and pyrite-like ditellurides are actually polymeric modifications leading to two new structural subgroups within these two families. A structures classification taking into account the dimensionality and the polymerization degree of such materials is suggested. A consequence of such anionic behavior is the occurrence of a partial oxidation state of tellurium, a frequent response of that element to a very stable cationic oxidation state. From many examples, it is shown that the polymerizing behavior of that heavy chalcogen anion seems to be much more general than expected and should lead to many charge transfer studies.

I. Introduction

Most transition elements react with chalcogen atoms to give MX_2 dichalcogenides (*1*). These phases have been extensively studied for several reasons. One of them is the large number of MX_2 compounds (X = S, Se, Te) exhibiting rather simple and similar (if not identical) structures, which allows one to understand the anion/cation interactions and to quantify them by relying on energy level considerations (*2*). Also, many phases present a layer (2D) structure leading to a very rich intercalation chemistry with many potential applications (*3*) and showing highly anisotropic physical properties, eventually resulting in charge density waves instabilities (*4*).

On the left of the Periodic Table, dichalcogenides show the layered structural arrangements of the TiS_2, NbS_2, or MoS_2 structure types, whereas on the right one finds three dimensional pyrite or marcasite structures (Table I). The frontier between 2D or 3D arrangements illustrates the destabilization of the higher oxidation states of the cation when moving from the left to the right of the Periodic Table, in relation to the progressively lowered cationic *d* electronic band levels. It appears, however, that most of the interest has been devoted to sulfides and selenides. Indeed, the loss of directionality of the bonds when reaching the bottom of a column (tellurium case) may favor three dimensional arrangements, as may also the decrease of electronegativity of the element, leading to an essentially anionic *sp* valence band higher in energy. On the other hand, a *d* cationic–*sp* anionic redox competition favored by the lowered *d* levels of the elements on the right of the Periodic Table, when at the same time tellurium shows the highest *sp* band, can lead to interesting features which make the study of the corresponding tellurides of particular interest. This paper presents some recent results obtained in the ditelluride family and illustrates the *sp* tendancy of the tellurium ions to give multiple anionic

0022-4596/92 $3.00

TABLE I

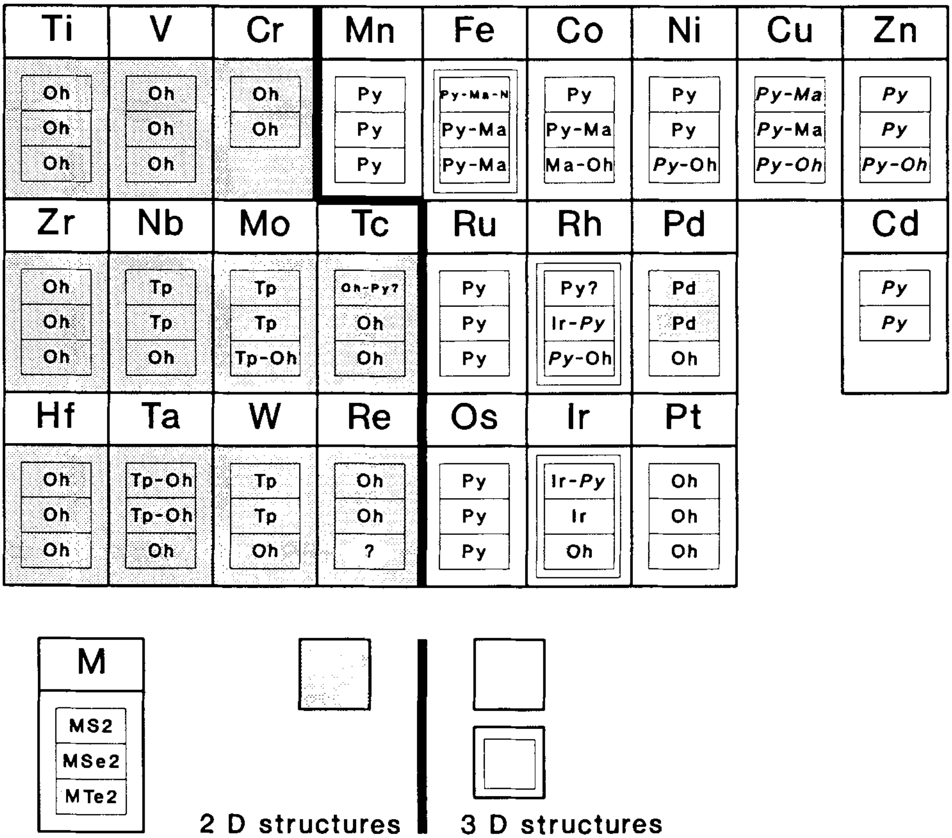

Ti	V	Cr	Mn	Fe	Co	Ni	Cu	Zn
Oh Oh Oh	Oh Oh Oh	Oh Oh	Py Py Py	Py-Ma-N Py-Ma Py-Ma	Py Py-Ma Ma-Oh	Py Py *Py*-Oh	*Py-Ma* *Py*-Ma *Py-Oh*	*Py* *Py* *Py-Oh*
Zr	**Nb**	**Mo**	**Tc**	**Ru**	**Rh**	**Pd**		**Cd**
Oh Oh Oh	Tp Tp Oh	Tp Tp Tp-Oh	Oh-Py? Oh Oh	Py Py Py	Py? Ir-*Py* *Py*-Oh	Pd Pd Oh		*Py* *Py*
Hf	**Ta**	**W**	**Re**	**Os**	**Ir**	**Pt**		
Oh Oh Oh	Tp-Oh Tp-Oh Oh	Tp Tp Oh	Oh Oh ?	Py Py Py	Ir-*Py* Ir Oh	Oh Oh Oh		

Note. Classification of the transition metal dichalcogenides MX_2 showing the separation (thick vertical line) between two dimensional phases (2D structures on left) and the mostly three dimensional phases (3D structures on right). For the 2D phases ($M^{4+}(X^{2-})_2$) (shaded on figure), octahedral (Oh) and trigonal prismatic (Tp) coordination of the cation is indicated, to be suppressed. In the predominantly 3D region, the PdS_2 and $PdSe_2$ phases exhibit a specific 2D arrangement (noted Pd), due to the special square coordination exerted by the palladium atom. Most of the 3D materials present a pyrite (Py) or marcasite (Ma) structural type ($M^{2+}(X)_2^{2-}$) or ($M^{+}(X_2)^{-}$) (bent letters indicate high pressure phases). A doubly framed area indicates the occurrence of special 3D structures ($M^{3+}X^{2-}(X_2)_{1/2}^{2-}$) with half the anions present as X_2 pairs, either of the $IrSe_2$ type (noted Ir) or of the new FeS_2 type (noted N), this last one being obtained by soft chemistry (see text). The Ir and N structural types differ from the nature of the cationic site (respectively Oh and Td).

bonds with low and fractional oxidation state, leading to polymeric networks.

II. The Structures of $IrTe_2$ and Ir_3Te_8. Extension to the MTe_2 Phases (M = Mn, Fe, Co, Ni, Cu, Rh, and Os)

(*A*) *IrTe*$_2$

The particular case of the IrX_2 family (X = S, Se) (5–7), in which the charge balance corresponds to the formulation $Ir^{3+}S^{2-}(S_2)^{2-}_{1/2}$, can be viewed not only as a cation/anion redox competition within the structure but also as a response of the chalcogen atoms to the very stable oxidation state (M^{3+}) of the transition metal. As far as the charge balance is concerned, it is a situation which is intermediary between the layered chalcogenides ($M^{4+}(S^{2-})_2$) and the tridimensional pyrite structures

TABLE II

PARAMETERS, c/a RATIO, VOLUME, INTERATOMIC DISTANCES, AND OXIDATION DEGREE OF TELLURIUM IN TRANSITION METAL DITELLURIDES WITH A CdI_2 AND POLYMERIC-CdI_2 STRUCTURE

Compound	$TiTe_2$	$ZrTe_2$	$HfTe_2$	$CoTe_{1.7}$	$RhTe_2$	$IrTe_2$	$NiTe_2$[a]	$PdTe_2$	$PtTe_2$	$CuTe_2$	$ZnTe_2$
a (Å)	3.757	3.950	3.949	3.802	3.92	3.928	3.855	4.037	4.026	3.95	3.98
c	6.513	6.630	6.651	5.411	5.41	5.405	5.256	5.126	5.221	5.49	5.25
c/a	1.733	1.680	1.68	1.42	1.38	1.38	1.36	1.27	1.30	1.39	1.32
V (Å^3)	79.61	89.58	89.92	67.71	72.0	72.23	67.67	72.33	73.28	74.18	72.02
$d^{(1)}_{Te-Te}$	3.913	4.025	4.032	3.446	3.53	3.498	3.429	3.487	3.464	3.56	3.49
$d^{(2)}_{Te-Te}$	—	—	—	3.521	—	3.558	3.461	3.441	3.526	—	—
$d^{(3)}_{Te-Te}$	3.757	3.950	3.949	3.802	3.92	3.928	3.854	4.036	4.025	3.95	3.98
d_{M-Te}	2.712	2.819	2.822	2.565	2.64	2.650	2.590	2.652	2.676	2.65	2.65
O.D.Te	(<2)	−2	−2	−1.2	−1.5	−1.5	−1.2	(−1.5)	(−1.5)	(−1)	(−1)
	← CdI_2 →			← CdI_2 polymeric →							

[a] Probably $NiTe_{2-x}$ (see text).

Note. $d^{(1)}_{Te-Te}$ refers to interslab Te–Te distances, $d^{(2)}_{Te-Te}$ to anion–anion distances belonging to the slab (on both sides of the transition element), *and* $d^{(3)}_{Te-Te}$ indicates tellurium atoms at the same elevation. Between brackets figures correspond to assumed oxidation states of tellurium (O.D.Te).

($M^{2+}(S_2)^{2-}$). With a more covalent character, tellurium is expected to present a similar behavior, since its valence band will be still higher in the ditelluride derivatives. Strangely, $IrTe_2$ was reported (*8*), until very recently, as exhibiting a CdI_2 layer structure. With the usual configuration, this would mean an Ir^{4+} cation, in contradiction with the less electronegative character of tellurium. The same structural type was reported for several other MTe_2 phases (M = Co, Ni, Cu, Zn, Rh, Pd, Pt) (*1*), although their disulfides and diselenides are pyrite or marcasite. It must be pointed out that for the eight members of that group, an anomaly appears concerning the cell parameters. In effect the c/a ratio is equal to about 1.37, a much lower ratio than the one reported for the phases with lighter chalcogens (ratio of c/a = 1.633 for ideal HC stacking) or for the element IVA tellurides (see Table II for the cell data on several MTe_2 compounds). In front of these obvious contradictions and questions, and because the behavior of the transition metal tellurides are often times so original and different from the other chalcogenides, a complete crystal and electronic structure determination of $IrTe_2$ was undertaken to elucidate the true nature of the phase (*9*).

Rietveld refinements made on that ditelluride (R_{wp} = 9.9 and R_{exp} = 7.6) showed at first the structure to belong to the CdI_2 type ($P\bar{3}m1$ space group). However, it was found that the tellurium ions located at different z elevations (0.2536 and 0.7464) were bonded to each other (d_{Te-Te} = 3.497 and 3.558 Å) (Fig. 1), whereas nonbonding anions at the same level were found at 3.928 Å, corresponding well enough to the sum of the van der Waals radii. Integrated atom–atom overlap population calculations at the Fermi level gave positive values (see Table III), demonstrating the true occurrence of Te–Te bonds. Because the tellurium atoms are not only bonded through the former van der Waals gaps but also through the structure slabs, a strong decrease of the stacking parameter follows (Fig. 1), explaining perfectly the small value of c and the low c/a ratio. $IrTe_2$ is hence not a layered phase but a three dimensional one, the former gap width falling from 3.29 Å in $ZrTe_2$ (*1*) and $HfTe_2$ (*1*), for instance, in these regular CdI_2-type structures to 2.66 Å in this phase. Figure 2 gives a perspective view of the 3D polymeric network constituted by the tellurium atoms in $IrTe_2$.

With an iridium cation 3+, the tellurium anions present an oxidation state of −1.5.

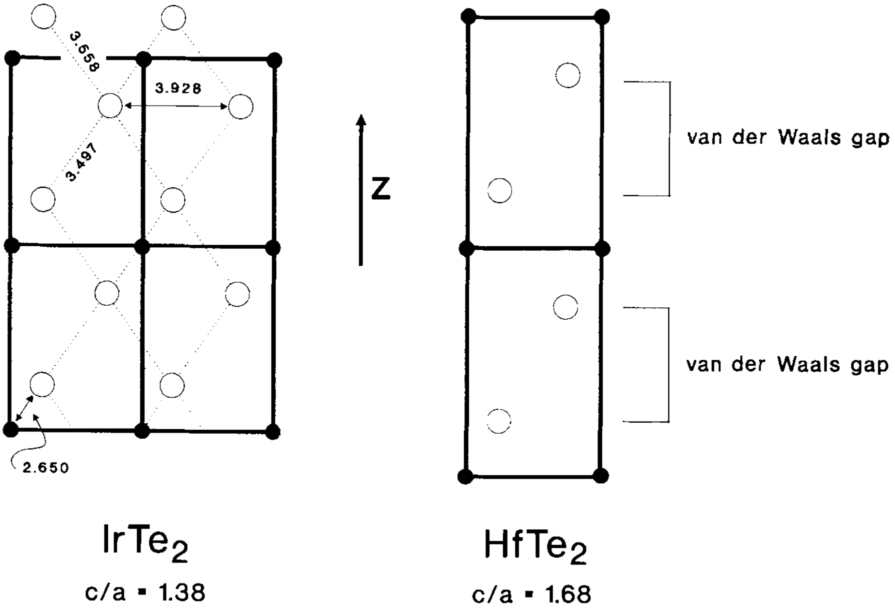

FIG. 1. (*11–20*) Plan section of the structure of polymeric $IrTe_2$ (a) and $HfTe_2$ (b) revealing the origin of the *c* axis difference (Te–Te bonds in the iridium phase).

Figure 3 shows a straight line variation of the Te–Te distances with respect to the anion oxidation states, in the case of Te^{2-} ($ZrTe_2$ and $HfTe_2$), $Te^{-1.5}$ ($IrTe_2$) (*9*), and Te^{-1} ($MnTe_2$) (*10*).

The two tellurium anions differ very little from each other, and this is revealed by the ESCA study made on the phase. Simple doublets at 583.3 and 573.0 eV are found for the two transitions, $5d_{3/2}$ and $5d_{5/2}$ (Fig. 4(a)). These values could be used as reference of an oxidation state of −1.5 for tellurium in the metallic state.

TABLE III

OVERLAP POPULATION AT THE FERMI LEVEL BETWEEN IRIDIUM–TELLURIUM, TELLURIUM–TELLURIUM AND IRIDIUM–IRIDIUM

Bonding type	Interatomic distance (Å)	Integrated overlap population
Ir–Te	2.650	+0.475
Te–Te	3.497 (gap)	+0.046
Te–Te	3.558 (slab)	+0.010
Te–Te	3.928	−0.010
Ir–Ir	3.928	−0.030

A generalization of these results to $CoTe_{2-x}$, $NiTe_2$, $CuTe_2$, $ZnTe_2$, $RhTe_2$, $PdTe_2$, and $PtTe_2$ can be done. Indeed, as shown in Table II, these materials present the same short Te–Te bonds. The difference of the cobalt and nickel derivatives compared to the iridium compound lies in the expected lower oxidation state for the metal, typically +2. The cobalt derivative is tellurium deficient, which is one possible answer to the charge decrease imposed by the cation to the anionic network ($Te^{-1.2}$). The nickel phase is reported stoichiometric, but its volume cell is identical to that of $CoTe_{1.7}$ (respectively 67.71 and 67.67 Å^3): it must thus be assumed that both phases have identical composition, and that syntheses and analytical work should be remade on this phase to confirm these findings. The occurrence of the same $Te^{-1.2}$ anions in the

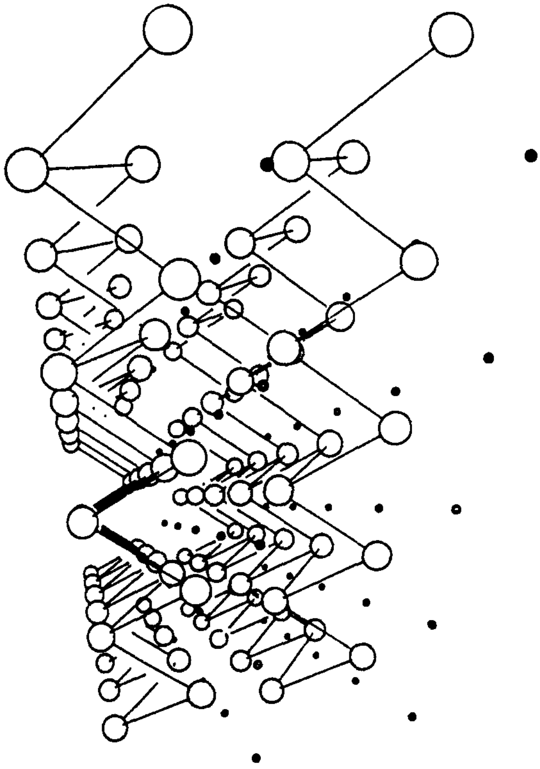

FIG. 2. Perspective drawing of 3D $IrTe_2$ showing the polymeric tellurium network.

structure is backed up by smaller $d_{Te\text{-}Te}$ distances of 3.483 Å as compared to the iridium phase ($d_{Te\text{-}Te}$ = 3.528 Å), in consistency with a decrease of the electronic population of antibonding levels of the tellurium network. Table II indicates the elements' oxidations states as deduced from physical measurements or as suggested from cell size considerations.

For the sake of comparison, the cell constants and anion distances of pure CdI_2-like phases are also reported. It is of interest to observe that whereas the zirconium and hafnium derivatives are almost ideal, $TiTe_2$ departs somewhat from the expected values with a rather short Te · · · Te in-plane distance (3.757 Å) and a too large c/a ratio. Since from Hf to Ti the d bands are progressively lowered, titanium may reach the limit point from which the $3d$ and $6p$ bands overlap, with a decrease of the titanium oxidation state, a correlative decrease of the anionic charge, and the occurrence of a weak Te–Te bond (the high c/a ratio (1.712) could be the indication of a Jahn–Teller d^1 effect due to some M^{3+} cations).

Clearly, all the MTe_2 phases under study belong to the same subgroup of the CdI_2-type, which can be called polymeric-CdI_2-type, not seen as such previously. A comparison with the IrS_2 structural type shows that the response of the anion to the cation oxidation state is twofold. In the IrS_2-type, the charges are distributed differently on two kinds of anions; in $IrTe_2$-type, the charges are evenly distributed through a polymeric 3D tellurium network.

It seems possible to draw a parallel between cationic and anionic behavior. Whereas the d^0 transition metal configuration in octahedral chalcogen coordination is rather stable, the d^1 to d^3 cations present some instability, leading frequently to metal–metal bonding (Fig. 5). Likewise, considering $(X_2)^{-3}$ hypothetical and isolated groups, one would have a configuration with a single electron, which is also rather unstable, although it can be observed in the case of $RhSe_2$. Stability is often reached through either disproportionation (X^{-2} and $(X_2)^{-2}$) as in IrS_2-type phases, or through the setting up of a polymeric network that maintains the same oxidation state on the anions ($(X_{2n})^{-3n}$) as in $IrTe_2$-type compounds. In both cases, the answer is the implementation of chalcogen–chalcogen bondings.

(*B*) Ir_3Te_8

Whereas some nonstoichiometry at the tellurium sites does not change the structure type, as in the case of the cobalt telluride, for example, metal deficiency in $IrTe_2$ (Ir_3Te_8) leads to the formation of a pyrite structure. In that case, the charge decrease reinforces one of the Te–Te bonds through electron depletion of a Te–Te antibond while weak-

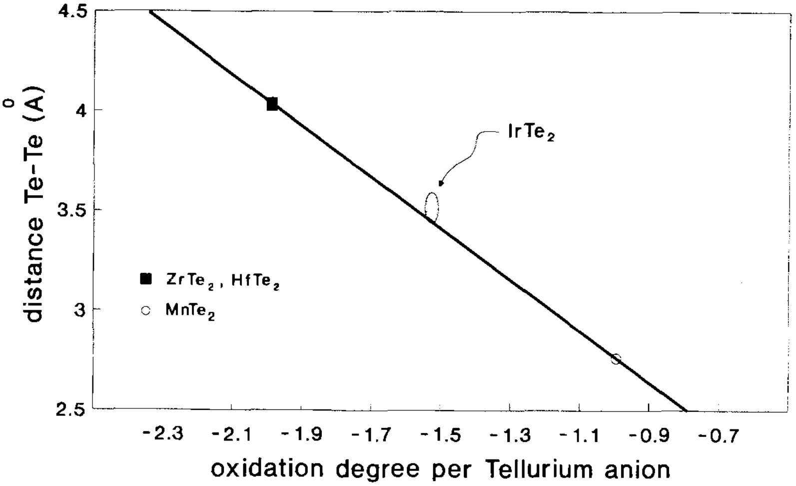

FIG. 3. Variation of the Te–Te distances versus the oxidation states of the anion in $(Te_2)^{2-}$, Te^{2-} demonstrating the occurrence of the oxidation state −1.5 of tellurium in $IrTe_2$.

ening the other one, leading to the formation of (Te_2) separated entities, in a scheme similar to the one proposed by J. K. Burdett and T. J. McLarnan (*11*) to explain, from a structural point of view, the transition from a 2D to a 3D type of structure. The reported cubic symmetry of Ir_3Te_8 (*8*) was shown to actually correspond to a trigonal one, and its structure was recently performed (*12*). Basically, the single crystal study ($R = R_w = 0.020$) shows the structure to be of the pyrite type with random distribution of Ir^{3+} on the cation sites. Te–Te pairs do exist, with a d_{Te-Te} distance of 2.833 Å to be compared to the same bonds in $MnTe_2$, for example (2.75 Å). However, looking at the inter-Te_2 pair distances of the structure, one finds some distances of 3.568 Å, very similar to those found in $IrTe_2$. These distances correspond to interpair bondings, as the important iridium deficiency implies a strong lowering of the tellurium charge achieved through the formation of these anionic linkings (because of the nonstoichiometry, no evidence of bonding could be given from extended Hückel calculations, but this was done on $FeTe_2$ with a Te · · · Te OP of 0.02). Since each tellurium of a pair is bonded to two others belonging to the same iridium coordination octahedron, this means that there exists here also a polymeric tellurium network within the Ir_3Te_8 structure, very much like in polymeric CdI_2-like $IrTe_2$, for which a distance of 3.53 Å corresponds to a bonding interaction. The charge borne per tellurium (−1.1) is smaller than that in $IrTe_2$, in agreement with the ESCA data that give for the $5d_{3/2}$ and $5d_{5/2}$ transitions, respectively, the values 583.8 and 573.5 eV, 0.5 eV smaller than for the same transitions in $IrTe_2$ (see Fig. 4(b)). A survey of reported pyrite-like telluride structures (*1, 10, 13*) (see Table IV) shows that all the phases, with the interesting exception of $MnTe_2$, present a polymeric pyrite type, with very short, medium, and long Te · · · Te distances, corresponding, respectively, to pairing, probably bonding, and nonbonding tellurium anions. True pyrite-like $MnTe_2$ shows a large jump of the volume per molecular weight from ca. 65 $Å^3$ for the polymeric compounds to ca. 84 $Å^3$, a difference indica-

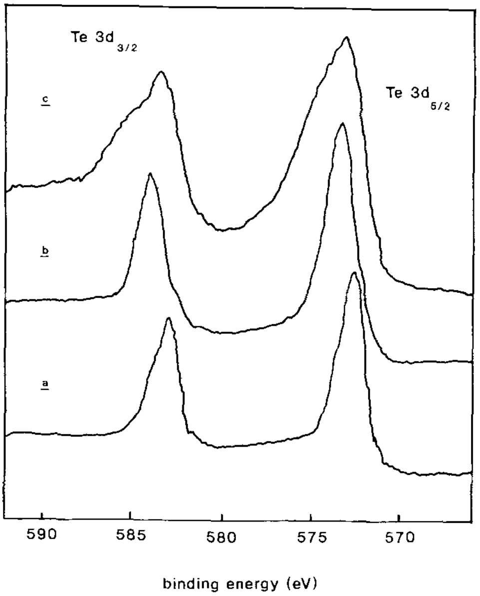

FIG. 4. (a) XPS spectrum of tellurium in $IrTe_2$ showing the two transitions $5d_{3/2}$ and $5d_{5/2}$; (b) the same in Ir_3Te_8; and (c) in $Cr_{2/3}Te_2$.

tive of truly noninteractive Te_2 pairs in the manganese phase. The same magnitude of difference could be also observed between true CdI_2 and polymeric CdI_2-true tellurides. It is worth noting that since the polymerization of the tellurium ions induces a lower anionic charge and corresponds to the same total decrease on the cation, this should mean a lower metal oxidation state; for instance, oxidation states lower than II are expected in $FeTe_2$ and $NiTe_2$, resulting in some sizeable transfer from the $(Te_2)^{2-}$, M^{2+} to $(Te_2)^{-2+\xi}$, $M^{+2-\xi}$ configuration. These observations are, however, not consistent with the interpretations of a Mössbauer study of ^{125}Te by H. Binczycka *et al.* (*14*) who, in the series $MnTe_2$ (pyrite), $FeTe_2$ and $CoTe_2$ (marcasite), and $NiTe_{2-x}$ (CdI_2 polymeric-like) suggest the respective cation effective charges of +2, +3, +3, and +4, in contradiction not only with the observations made in the previous paragraph, but also with the progressive lowering of the transition metal *d* bands from Mn to Ni and the more and more reducing property of the top of the anionic band.

III. The Anionic Mixed Valence and Layered $Cr_{2/3}Te_2$

As seen before, the tellurium anions adapt themselves, through change in their oxidation states, i.e. homobonding or catenation, to respond to the charge borne by the cations. It seems that in some cases, like $FeTe_2$ and $NiTe_2$, adjustments are made through extra bonding overlaps with a departure from the regular and round oxidation state figures. We are now going to look at a phase for which one may wonder whether the proposed charge balance is as simple as it appears, or if it is more complex with undetected anionic level mixings.

$CrTe_3$ presents a charge balance that can be readily understood and accepted according to the structural work done by K. O. Kepp and H. Ipser (*15*). That phase has a layered structure whose sheets consist of building groups of four edge-linked ($CrTe_6$)-octahedra which are connected via apical tellurium atoms to give a two-dimensional infinite arrangement. In addition, these building groups are linked together via Te–Te bonds, giving rise to the formation of Te_2 and Te_3 entities (Fig. 6(a)). In that phase, very stable Cr^{3+} imposes a mean oxidation state of −1 on the tellurium anions which is achieved as follows: $[Cr^{3+}]_2[Te^{2-}][Te_2]^{2-}[Te_3]^{2-}$. To the polyanions correspond intra-atomic distances of 2.816 and 2.824 Å for Te_3 and 2.817 Å in Te_2. Although somewhat longer than in regular $M^{2+}(Te_2)^{2-}$ (2.616 to 2.789 Å), these values fall in the expected range for Te–Te bonds. The tellurium distances on each side of the van der Waals gap reveal no bonds (3.857 Å $< d_{Te-Te} <$ 3.946 Å) (Fig. 6(b)), but, inside the structure sheets, distances around 3.430

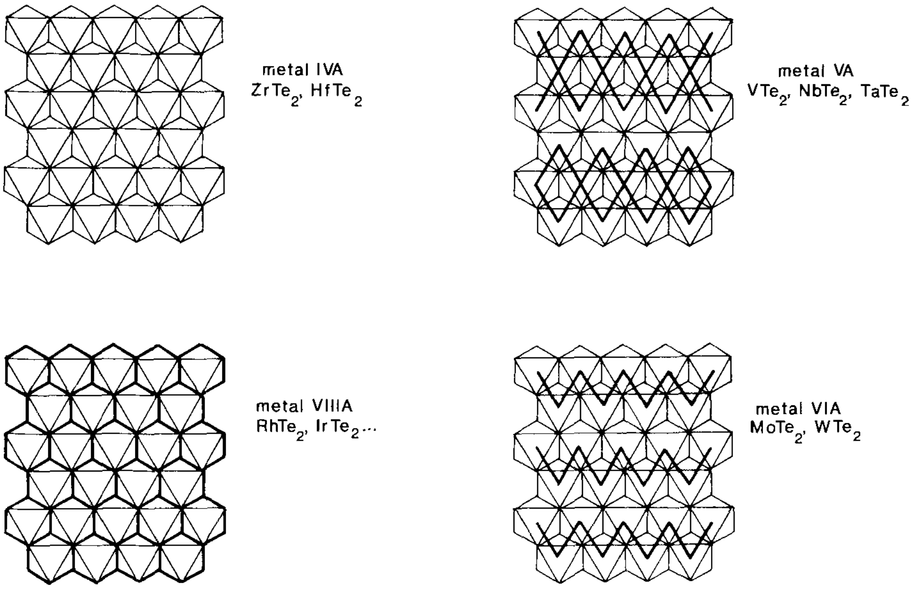

FIG. 5. Distortion of the CdI$_2$ structure when M belongs to IVA, VA, VIA, and VIIIA metal transition subgroups. For VTe$_2$, NbTe$_2$, and TaTe$_2$ we observe weak M–M bonding which forms double zig-zag chains. For MoTe$_2$ and WTe$_2$, the M–M bonding is more pronounced and we observe zig-zag chains. For VIIIA elements, we have a polymerization of the tellurium network.

Å are calculated, posing the question of weak tellurium bondings of the type existing in the phases studied in the previous chapter. A compete examination of the structure shows that within the *bc* plane of the layers, all the anions and polyanions are at close range (all distances between 3.437 and 3.507 Å), allowing a possible bonding percolation throughout the 2D planes. In the hypothesis of actual bonds, this would result in the occurrence of a polymeric 2D network and would correspond to truly polymeric and layered phase at the same time. To prove it, this prompted a series of physical measurements and band calculations.

If the many interanionic short distances are of bonding character, a metallic behavior could be expected with possible electronic instability in relation to the 2D structure. Conductivity measurements showed that the phase is in fact semiconducting ($E_A = 0.35$ eV), in agreement with the rather flat features of the electronic bands (*16*). The magnetic susceptibility measured versus temperature in the 300–500 K range allowed us to determine the spin state of the chromium ions: it is a Cr^{3+} with a d^3 configuration. The Cr^{3+} state is also demonstrated by the Cr–Te distances that yield a mean distance of 2.728 Å, giving a chromium ion size (with an effective radius $R^{2-}_{\mathrm{Te(IR)}} = 2.10$ Å) of 0.63 Å, in agreement with that of 0.62 Å compiled by Shannon (*17*) in chalcogenide phases for Cr^{3+} in octahedral environment (a value of 0.68 Å is found in layered and structurally related CrSiTe$_3$ for the same ion) (*18*). In the assumption of interbonded tellurium groups, one expects a priori a lowering of the anionic charges and a lowering also of the oxidation state of chromium. This is not observed here. However, semiquantitative orbital population calculations (*16*) give positive values (about 0.02) between close tellurium belonging to neighbor Te$_3$

TABLE IV

LATTICE PARAMETERS, VOLUME PER MTe$_2$, MAIN INTERATOMIC DISTANCES AND OXIDATION DEGREE OF TELLURIUM IN CLASSICAL AND POLYMERIC MTe$_2$ PYRITE STRUCTURES

Compound	Parameter (Å)	Volume/MTe$_2$ (Å^3)	d(M–Te) (Å)	d(Te–Te) (Å)	O.D.Te
$MnTe_2$	6.951	83.95	2.907	**2.750** 3.955 4.262	−1
$FeTe_2$[a]	6.294	62.32	2.619	**2.626** 3.547 3.855	<−1
$NiTe_2$[a]	3.374	64.75	2.653	**2.650** 3.592 3.904	<−1
$CuTe_2$[a]	6.605	72.05	2.749	**2.746** 3.722 4.046	?
$RuTe_2$	6.391	65.25	2.648	**2.790** 3.567 3.914	<−1
$RhTe_2$	6.448	67.02	2.659	**2.969** 3.560 3.951	−1.5
$OsTe_2$	6.397	65.45	2.647	**2.830** 3.561 3.918	<−1
Ir_3Te_8	6.411	65.88	2.653	**2.883** 3.568 3.926	−1.1

Note. Bold and underlined figures relate to the Te_2 pairs and to Te–Te interactions interpairs, respectively.

[a] Distances calculated with a classical fractional coordinate x value of 0.38.

chains (3.506 Å distance), whereas the other values are much lower and probably too weak to correspond to bonding. This bridge between the Te_3 polyanions set up infinite chains parallel to the bc plane in the c direction. With that example it seems that one has a polymeric 1D anionic system. In the assumption of the polymerization of the Te_3 groups, one has then to consider a small negative charge transfer on the Te_3 1D files themselves, without involving the cation. $CrTe_3$ is thus again a case in which very stable Cr^{3+} imposes complex mixed valences upon the tellurium atoms. This creates strong distortions in the structure (hence the longer Te–Te bond length in the Te_2 and Te_3 groups mentioned before, in this latter case that bond lengthening can be increased by some intergroup transfer), with implementation of selective weak Te–Te bonds. One has here a situation quite original compared to the other ditellurides studied above. The charge balance straightforwardly written from the structure determination seems to be only a broad approach. With three well identified types of tellurium anions, one could expect three separated ESCA transitions. Experiments actually could not easily differentiate between the different oxidation states, although a widening of the peaks from 573 to 575 eV for the $5d_{5/2}$ transitions could be observed (Fig. 4(c)).

The necessity to put up extra Te–Te bonds

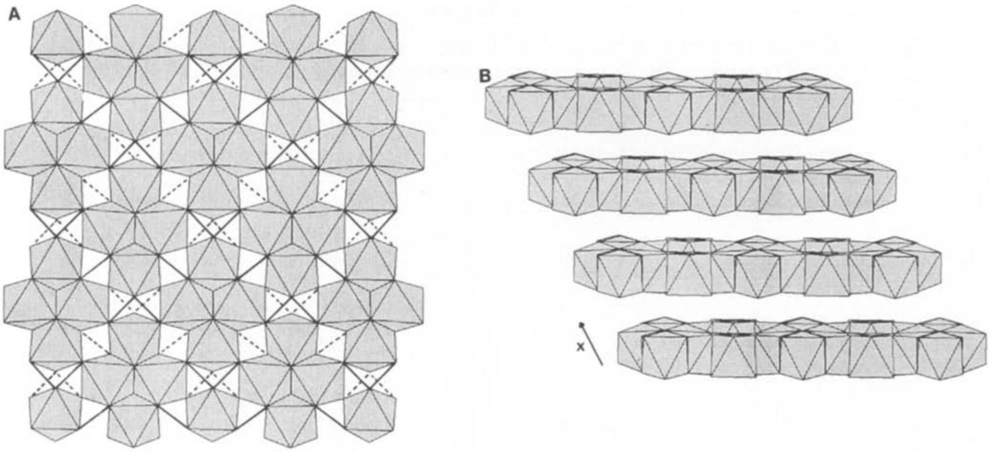

FIG. 6. (a) Projection, in the (*bc*) plane, of the structure of $Cr_{2/3}\square_{1/3}Te_2$. The phase is built from four edge sharing octahedra linked through apical tellurium and Te–Te and Te–Te–Te groups. (b) Perspective drawing of $Cr_{2/3}\square_{1/3}Te_2$ showing the layered feature of the phase; between ($Te–Cr_{2/3}\square_{1/3}–Te$) planes, no Te–Te bonds exist.

in a low-dimensional structure can easily be achieved, at little energy distortion cost, through the van der Waals gap of the structure. In effect, bonding overlap and polymerization can probably be easily achieved by the tellurium *p* orbitals through the gap rather than within the slabs, in relation with symmetry and orientation conditions. From that simple observation, it can be inferred that any short Te · · · Te distances across a gap will be a good indication of bondings and of polymerization within a given low-dimensional structure. Other short distances will have necessarily to be subjected, whenever possible, to electronic overlap population calculations and appropriate physical measurements to prove their bonding nature and discuss the charge transfers.

IV. Conclusion: Dimensionality and Polymerization

The chemistry of tellurides is, for a large part, driven by the particular behavior of tellurium which, with its particular size and redox properties, in relation to its band level positions respective to the metal *d* orbital ones, leads to many varied anionic groupings. Until recently, the difference between true two dimensional and two dimensional-derived polymerized phases was not really made. Also, the occurrence of extrabonding within three dimensional arrangements like the pyrite-type phases introduces polymerization as an extra structural factor within already 3D phases. Obviously, these new observations lead to the distinction between dimensionality and polymerization, in order to classify the transition metal ditellurides, and beyond them, all the other tellurium-containing phases. Table V shows a classification taking into account the phase dimensionality (2D and 3D) and, within each domain, the degree of polymerization, i.e., the number of directions and ways in which tellurium bondings create polymeric networks. The degree of polymerization (from 0 to 4) may maintain 2D structures when tellurium bondings take place within the slabs (along *a*, *b*, *c*, or *G* (through gap)). Bonding through the van der Waals gap of a layered phase gives polymeric 2D-derived

TABLE V

MTe$_2$ PHASES

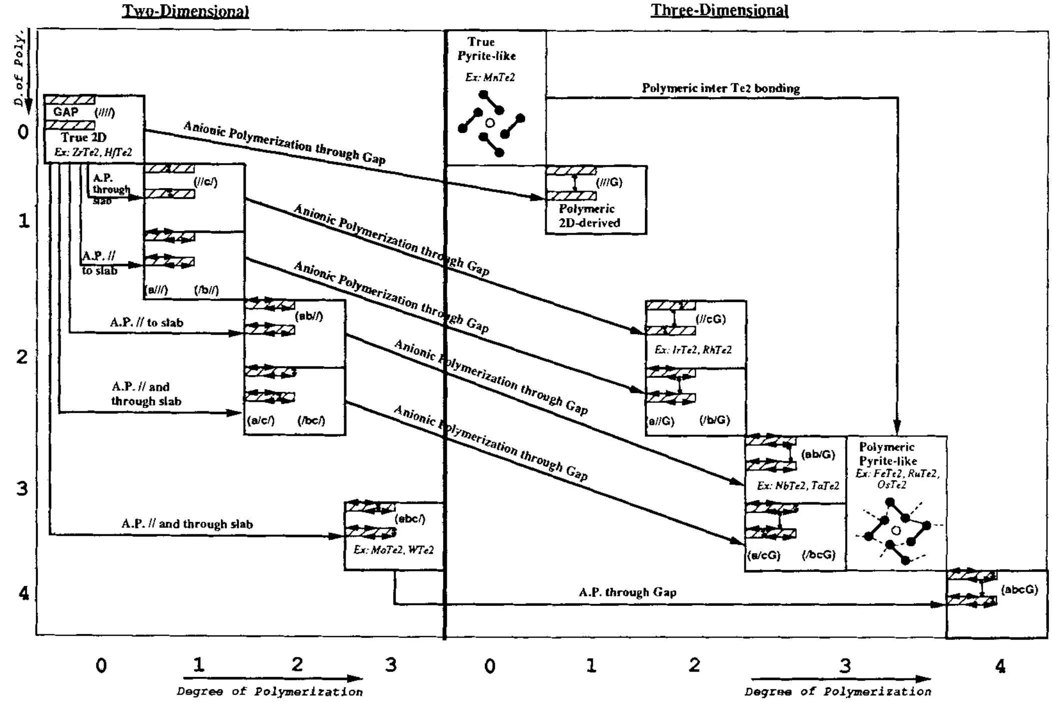

Note. Classification of ditellurides taking into account not only the dimensionality of the phases but also the polymerization degree (from 0 to 4) of the tellurium network (arrows indicate the direction of anionic bonding (*a*, *b*, *c* (slab), gap)).

compounds and locates the corresponding phases within the three dimensional domain. 3D compounds undergoing polymerization maintain the phases into the same domain but with a displacement along the diagram axes. Going through the different ditellurides known and classifiable to date, one can make the following comments:

(*A*) *In the Two-Dimensional Domain*

1. True 2D phases are represented by $TiTe_2$, $ZrTe_2$, and $HfTe_2$.

2. Within the in-layer polymeric 2D phases domain (left lower part of Table V), through and within-layer bondings seem to be the case of WTe_2 and $MoTe_2$ (*19*) (distances of 3.679 and 3.520 Å on the one hand and 3.652, 3.671 Å and 3.493 Å on the other hand are given for within- and through-layer tellurium distances, respectively, for WTe_2 and $MoTe_2$). Of course, as explained before, actual bondings should be proved by physical experiments and calculation. Within layer, 1D polymerization is to be found in $Cr_{2/3}\square_{1/3}Te_2$.

(*B*) *In the Three-Dimensional Domain*

3. True pyrite-like phases ($MnTe_2$ for instance) (zero degree of polymerization) give rise to polymeric pyrite-like phases exemplified by $FeTe_2$, $NiTe_2$, $RuTe_2$, etc., as shown in this article.

4. 3D polymeric 2D-derived phases like $IrTe_2$, $RhTe_2$, $CoTe_{1.7}$, etc., obtained from

two dimensional models present two degrees of polymerization (through-layer and through-gap).

5. 3D polymeric 2D-derived compounds with also two degrees of polymerization (parallel to layer and through-gap) can be found. This family can probably be represented by $NbTe_2$ and $TaTe_2$ (*20*) with parallel to layers Te· · ·Te distances of 3.560 and 3.558 Å for $NbTe_2$ and $TaTe_2$, and through-layer lengths of 3.527, 3.600, and 3.595, 3.651 Å. Again there is no true evidence, to our knowledge, of bonding in these phases. However, contrary to the case of WTe_2 and $MoTe_2$ mentioned before, we have here an example of short through-gap distances which do not seem to be implied by internal structural strain. In that case, one may assume true anionic bonding pending confirmation through physical measurements.

Although not many complex transition metal tellurides are known to date, several layered ternary compounds were recently made and their structures determined in the $MM'Te_5$ family with M = Nb, Ta and M' = Ni, Pd, for instance (*21–23*). It is of interest to note that very short Te· · ·Te distances of 3.196 Å were calculated. In addition, the magnetic moment obtained for $NbNiTe_5$ (μ_{eff} = 1.24 B.M.) implies a complex and unusual charge transfer between the anions and the metal atoms, as evidenced from the compound formula: with five tellurium and a maximum of seven positive charges (Nb^{5+} and Ni^{2+}), tellurium anions must have fractional oxidation state and, according to the observations made above, polymerization is expected. There is no doubt that many tellurides to be synthesized in future works will pose the same and interesting problem of actual charge transfer.

References

1. (*a*) R. M. A. Lieth, Ed., "Preparation and Crystal Growth of Materials with Layered Structures," Kluwer, Boston (1978); (*b*) F. Levy, Ed., "Crystallography and Crystal Chemistry of Materials with Layered Structures," Kluwer, Boston (1975); (*c*) Fritz Hulliger, *in* "Structural Chemistry of Layer Type Phases," (F. Levy, Ed.), Physics and Chemistry of Materials with Layered Structures, D. Reidel Publishing Co., Dordrech, Holland/Boston (1976/77).

2. (*a*) C. F. van Bruggen, *Ann. Chim. Fr.* **7,** 171 (1982); (*b*) J. C. W. Folmer, J. Jellinek, and J. H. M. Calis, *J. Solid State Chem.* **72,** 137 (1988).

3. (*a*) M. S. Whittingham, *Prog. Solid State Chem.* **12,** 41 (1978); (*b*) D. W. Murphy, J. Broadhead, and B. C. H. Steele, Eds., "Material for Advanced Battery," Plenum Press, NY (1980); (*c*) J. Rouxel, *in* "Intercalated Layered Materials," (F. Lévy Ed.), pp. 201–250, D. Reidel Publishing Co., Dordrecht, Holland (1979); (*d*) J. Rouxel, "Physical Chemistry of Intercalation Reactions," Nato Asi, Bonas (1987); (*e*) R. Brec and J. Rouxel, *NATO ASI, Serie B:* **148,** 75 (1987).

4. L. Gorkov and G. Grüner, Eds., "Charge Density Waves," Northland (1990).

5. L. B. Barricelli, *Acta Crystallogr.* **11,** 75 (1958).

6. S. Jobic, P. Deniard, R. Brec, J. Rouxel, M. G. B. Drew, and W. I. F. David, *J. Solid State Chem.* **89,** 315 (1990).

7. F. Hulliger, *Nature (London)* **204,** 644 (1964).

8. E. F. Hocking and J. G. White, *J. Phys. Chem.* **64,** 1042 (1960).

9. S. Jobic, P. Deniard, R. Brec, J. Rouxel, A. Jouanneaux, and A. N. Fitch, *Z. Anorg. Chem.*, in press.

10. N. Elliott, *J. Am. Chem. Soc.* **59,** 1958 (1937).

11. J. K. Burdett and T. J. McLarnan, *Inorg. Chem.* **21,** 1119 (1982).

12. S. Jobic, M. Evain, R. Brec, P. Deniard, A. Jouanneaux, and J. Rouxel, submitted for publication.

13. G. Brostingen and A. Kjehshus, *Acta Chem. Scand.* **24,** 2993 (1970).

14. H. Binczycka, S. S. Hafner, G. Moh, and J. Stanek, *Phys. Lett. A* **145,** 467 (1990).

15. K. O. Kepp and H. Ipser, *Angew. Chem. Int. Ed. Engl.* **21,** 911 (1982).

16. E. Canadell, S. Jobic, and R. Brec, *J. Solid State Chem.*, in press.

17. R. D. Shannon, *Acta Crystallogr., Sect. A: Found. Crystallogr.* **32,** 751 (1976).

18. G. Ouvard, E. Sandre, and R. Brec, *J. Solid State Chem.* **73,** 27 (1988).

19. B. E. Brown, *Acta Crystallogr.* **20,** 268 (1966).

20. B. E. Brown, *Acta Crystallogr.* **20,** 264 (1966).

21. E. W. Liimatta and J. A. Ibers, *J. Solid State Chem.* **71,** 384 (1987).

22. E. W. Liimatta and J. A. Ibers, *J. Solid State Chem.* **77,** 141 (1988).

23. E. W. Liimatta and J. A. Ibers, *J. Solid State Chem.* **78,** 7 (1989).